



# The William Blum Lectures

#57 – Timothy D. Hall – 2023



The 57<sup>th</sup> William Blum Lecture  
Presented at NASF SUR/FIN 2023  
in Cleveland, Ohio  
June 8, 2023

## Practical Observations in Surface Chemistry and Boundary Layer Control to Enable Scalable Electrochemical Operation

by  
Dr. Timothy D. Hall  
Recipient of the 2023 William Blum  
NASF Scientific Achievement Award





# The William Blum Lectures

#57 – Timothy D. Hall – 2023

The 57<sup>th</sup> William Blum Lecture

Presented at NASF SUR/FIN 2023

in Cleveland, Ohio

June 8, 2023

## Practical Observations in Surface Chemistry And Boundary Layer Control to Enable Scalable Electrochemical Operation

by

Dr. Timothy D. Hall

(Faraday Technology, Inc., Clayton, Ohio, USA)

Recipient of the 2023 William Blum

NASF Scientific Achievement Award

**Editor's Note:** The following paper is based on Dr. Hall's William Blum Memorial Lecture at SUR/FIN 2023, in Cleveland, Ohio on June 8, 2023. Dr. Hall was announced as the recipient of the 2023 NASF William Blum Scientific Achievement Award at the Cleveland, Ohio conference.

**Author's / Employer's Note:** At Faraday Technology, Inc., (Clayton, Ohio), the inherent breadth of boundary layer and surface chemistry control that can be achieved has been realized for numerous applications across various sectors. Note, the approaches and observations discussed herein have either been published, patented or have pending patents associated with the approach. These patents align with our business model, which is to provide our customers the opportunity to adopt and license new technologies that can improve process robustness and product quality, reduce chemical use/maintenance, lower cost and improve throughput.

### ABSTRACT

*This paper focuses on the practical effects of controlling the boundary and surface chemistry on a wide range of electrochemical applications. After a brief introduction to the concept and principles of surface and boundary layer properties during electrochemical processes, I discuss the use of this approach in controlling various physical properties during electroplating and electrochemical finishing. This includes controlling coating stress and metal composition, as well as enabling simple water-based electrolytes to polish passive or complex materials.*

### 1. Introduction

After it was announced that I was the recipient of the 2023 Scientific Achievement Award, named in honor of William Blum, I was extremely surprised and humbled. As with any of the previous winners, I recognize that this award is a credit to all the people I have had the pleasure to work for or with over my time in the industry. These mentors, colleagues and collaborators have enabled new perturbations in understanding and refined my intuition for a large range of electrochemical systems. Because of their critical impact on this and all the work of which I have graciously been a part, I hope to acknowledge all my colleagues/collaborators at the conclusion of this manuscript.

My first introduction to electrochemistry was as an undergraduate student while conducting research at West Virginia University. I carried these experiences into my graduate work at the University of Notre Dame, into my first job at NuVant Systems Inc., and finally to Faraday Technology Inc. where I have had the pleasure of spending the last 15 years.

### 2. Considerations of Changes at or Near an Electrochemical Surface

During electrochemical operations there are several simultaneous phenomena occurring. These include:

- Oxidation/Reduction: Oxidation (of the surface) or reduction of a species at or near the surface [Note: These changes result in modification of the chemical makeup and structure of the surface.];
  - Oxidation:  $M^0 \rightarrow M^+ + e^-$  (1)
  - Reduction:  $M^+ + e^- \rightarrow M^0$  (2)
- Diffusion: The consumption or creation of materials at the surface of the electrode create diffuse boundary layers driven by the local concentration gradient of the limited species [Figures 1 and 2 (Green layer) represent electroplating and surface finishing processes, respectively.] and;
- pH: Local pH changes as a result of water electrolysis (between the Stern ( $H^+$  rich; Equation 3) and Debye layers ( $OH^-$  rich; Equation 4) in the Nernst Diffusion layer) [Figure 1 - Blue layer; for an electroplating process].

#### 2.1. Electroplating (Electrodeposition)

At the cathode:



Figure 1 shows a generalized electrochemical model of electroplating. Simultaneous reduction of a metal onto the cathode surface and electrolysis of water creates both a low metal concentration and a high pH near the cathode surface, respectively.

Conventional plating operations use complex chemistries that enable control of diffusion through the boundary layer and the reduction processes (including water electrolysis) that happen at the surface. In Faraday's case, we typically reduce the number of additives by using pulsed electric field to control the thickness, concentration of species, and pH of the boundary layer. Knowing these factors, you can begin to anticipate the behaviors of the resulting reduction products. Below, in "Case Studies in Electroplating," we discuss approaches to predict and plan electrochemical process operations to achieve the targeted application of metals and alloys.

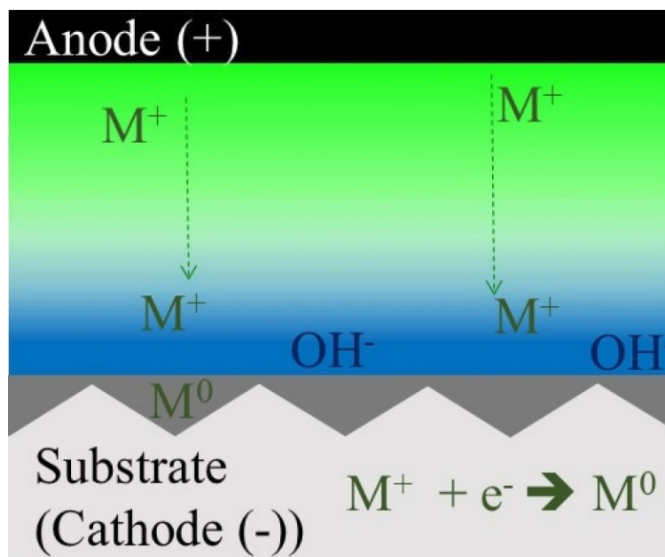


Figure 1 - Illustration that highlights reduction at the cathode during an electroplating process. Electrolysis of water (which occurs during low current efficiency deposition) results in a high pH (blue) near the electrode surface. A diffusion boundary layer (green) forms due to reduction of the metal ions near the surface. The deposited metal ( $M^0$ ) is represented by the dark gray.

#### 2.2. Surface Finishing (Electrochemical Machining/ Electrochemical Polishing)

Conventional electrochemical surface finishing relies heavily on the chemistry of the electrolyte to control the formation and diffusion of the solubilized, hydrolyzed or dissolved metal ions from the anode surface to the bulk electrolyte. Figure 2 shows an exemplar operation in which a metal ( $M$ ) is dissolved ( $M^+$ ), and then diffuses into the bulk electrolyte. The high metal concentration near the surface changes the local resistances between the anode and cathode; the recesses see a higher resistance ( $\Omega_r$ ) than the peaks ( $\Omega_p$ ) and therefore current is focused on the peaks (per Jacquet's Model (1936)<sup>1</sup>). The required diffusion control to enable local resistivity changes is the key feature that defines the electrolyte used in conventional processes.

Generally, viscous, low-temperature electrolytes are used with minimal flow to control the diffusion of the dissolved metal from the surface of the anode. In the case of conductive water-based electrolytes, the thickness of the boundary layer is controlled by

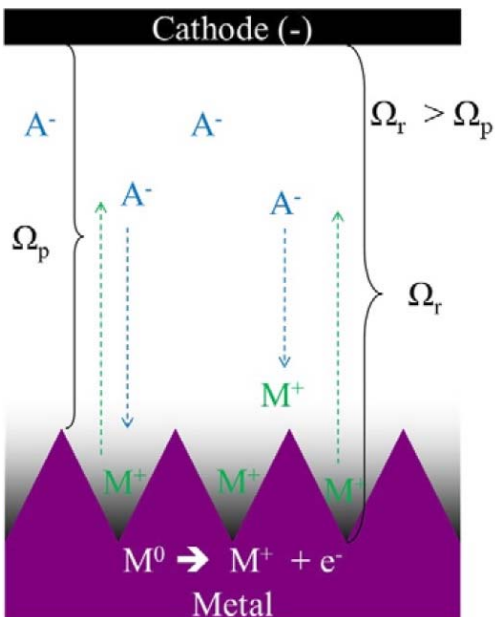


Figure 2 – Representation of Jacquet's model, where the metal substrate dissolves, creating a metal-rich layer in the valleys of the substrate ( $M^+$ ). This metal-rich layer increases the resistance ( $\Omega_r$ ), enabling focused dissolution on the peaks of the surface, which have a lower resistance ( $\Omega_p$ ).

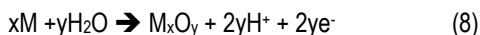
flow rate, the rate of material removal (*i.e.*, current density) and the rate of diffusivity. The following studies give examples of how the roughness of the material can directly affect the achievable surface finish, and how you can work around that restriction by controlling these variables.

The key difference between electroplating and surface finishing operations is that in electroplating, you are targeting and controlling specific reduction pathways with your process and your chemistry, while in surface finishing the oxidation reaction is less controlled and can take various electrochemical pathways leading to multiple oxidation, hydration and precipitation states. Additionally, as highlighted in Figure 2, the metal ion concentration is higher nearer the anode surface, and more diffuse in the bulk electrolyte.

For example, the elements of the anode can:

- Solubilize at the surface and then diffuse out into the bulk electrolyte as a metal ion (Equation 5);
- Solubilize at the surface and then precipitate (due to the presence of  $OH^-$  from water electrolysis (Equation 6)) in the boundary layer as a metal hydroxide (Equation 7). Note: The resulting metal hydroxide can then either: (1) stick to the anode or (2) create a separate diffusion gradient, because the diffusion of the bulky metal hydroxide precipitate is generally significantly slower.
- Passivate (oxidize) at the surface as a metal oxide (Equation 8); Note: These oxides are generally insoluble and can shut down surface finishing operations, due to lack of conductivity).

At the anode:



Considering that most surface finishing operations are performed on metal alloys (wrought or additive), rather than pure metals, you need to consider how each element of the alloy will behave during oxidation. This behavior is dependent on the chemistry and pH of the electrolyte. Knowing these factors, you can begin to anticipate the behaviors of the resulting oxidation products. Below, in "Case Studies in Electrochemical Surface Finishing," we discuss approaches to predict and plan electrochemical process operations to achieve the targeted surface modifications.

### 3. Case Studies in Electroplating

#### 3.1. Single Metals

In a 2020 study, we found that the electrodeposition of chromium (Cr) from a trivalent electrolyte can only be achieved at very low current efficiencies (7 to 20%, depending on the operating conditions).<sup>2</sup> These low current efficiencies lead to a large amount of water electrolysis, which results in a local increase in the electrolyte pH from 2.5 (in the bulk) to close to 10+ near the

surface of the cathode. At this pH, the Cr in the electrolyte begins to chemically precipitate (as  $\text{Cr}(\text{OH})_3$ ),<sup>3</sup> which can be incorporated into the Cr deposit. Furthermore, the carbon-based complexors used in the electrolyte break down at the high current densities typically used in the electroplating process, leading to the formation of Cr-C (carbides and hydrides) that can also be incorporated into the deposit. The incorporation of these carbon-based inclusions creates compressive stresses in the Cr deposit, as previously discussed and reprinted here in Figure 3.<sup>2</sup>

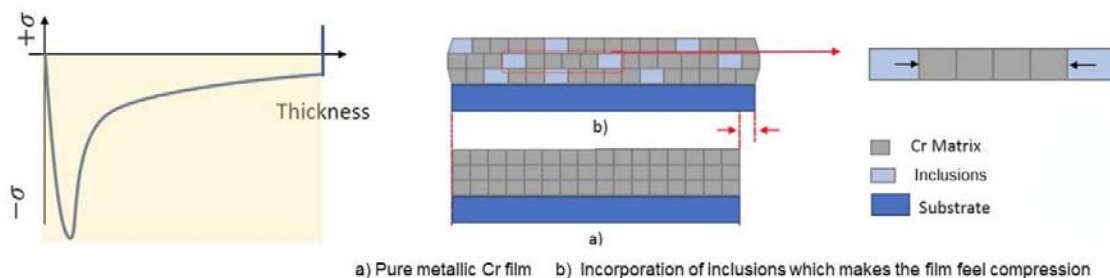


Figure 3 - An inclusion-based conceptual model of how compressive stresses form during the deposition of Cr from the trivalent chromium electrolyte.

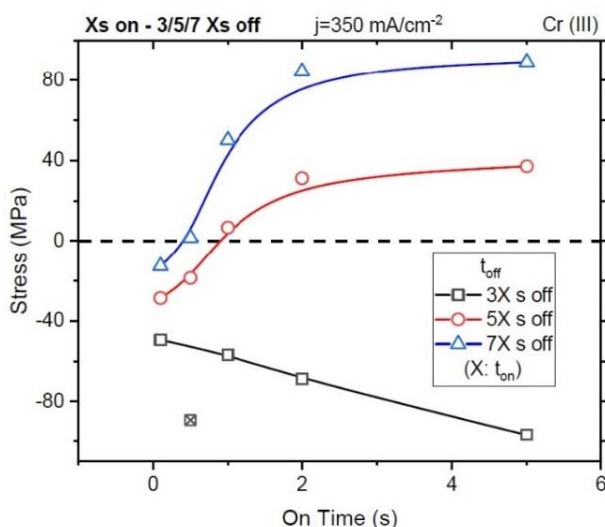


Figure 4 - Total stress observed in the coating after applying waveform conditions with controlled on-times and specified off-times.

The 2020 study showed that by using a pulsed electric field to electroplate the Cr deposit, the compressive stress formed in the deposit could be reduced or eliminated (as highlighted in Figure 4). The addition of off-times in the pulsed waveform, 5 to 7 times proportionally longer than the pulse on-times, led to a reduction/removal of the compressive stress in the Cr deposit. It is speculated that this reduction in internal stress was due to a lower average pH near the surface, the partial dissolution of the Cr hydrides/hydroxides, and diffusion of formed carbides from the surface. The combination of these mechanisms led to Cr deposits with improved microstructure and physical properties.

### 3.2. Alloy Metals

Faraday has demonstrated the ability to electroplate a functionally graded NiMo alloy coating onto a 316H SS substrate from a single electrolyte, by controlling the electroplating conditions and the current density (This work is disclosed in US Patent Application # 63/502,767.<sup>4</sup>). The NiMo electrolyte consisted of 0.20M Ni from nickel sulfate

hexahydrate ( $\text{NiSO}_4 \cdot 6\text{H}_2\text{O}$ ), 0.18M sodium citrate dihydrate ( $\text{Na}_3\text{C}_6\text{H}_5\text{O}_7 \cdot 2\text{H}_2\text{O}$ ) and 0.01M Mo from sodium molybdate dihydrate ( $\text{Na}_2\text{MoO}_4 \cdot 2\text{H}_2\text{O}$ ), with the addition of ammonium hydroxide to reach an electrolyte pH of 9. NiMo was electroplated onto 316H SS using a sequence of pulse-reverse waveform conditions. After application of the functionally graded NiMo coating, the samples were air dried and characterized using scanning electron microscopy (SEM) image with an energy dispersive X-ray spectroscopy (EDS) line scan. Figure 5 shows a cross-section of the NiMo alloy coating, from the surface to the 316H SS substrate. The concentration of Ni (blue line) and Mo (orange line) (by EDS) was controlled through the thickness of the deposit.

Specifically, the coating composition was ~80 wt% Ni at the substrate/coating interface to about ~55 wt% Ni at the surface of the coating. Figure 5 shows the change occurring over about 250  $\mu\text{m}$ . Faraday has demonstrated similar changes over larger (1 mm) or smaller thicknesses (<50  $\mu\text{m}$ ).

### 4. Case Studies in Electrochemical Surface finishing

#### 4.1. Stainless Steel

Polishing of (300 Series) stainless steels is typically accomplished via a two-step surface finishing approach. The first is generally a mechanical approach (*i.e.*, abrasive flow machining) to reduce the tool lines and overall,  $R_a$  from component manufacturing, while the second is conventional electropolishing to achieve the final mirror-like surface finish. The conventional electropolishing process uses a chilled electrolyte solution consisting of concentrated sulfuric/phosphoric acid as well as proprietary additives. This electropolishing process required ~160 seconds to achieve the final mirror-like finish.

In our case, we demonstrated an aqueous NaCl/NaNO<sub>3</sub> electrolyte that could perform both actions, enabling tool line removal and the final finishing with a single setup. The primary challenge with electropolishing SS with neutral salts is that the dissolution of Fe, Ni and Cr occurs simultaneously with the formation of hydroxides (specifically Fe(OH)<sub>2</sub>) that precipitate near the surface during operation. These precipitates are necessary to achieve finishing (due to their control over the boundary layer), but also lead to challenges, due to their tendency to stick to the anode surface and be sensitive to the availability of electrolyte flow. The control of the mobility, density and adhesion of the hydroxides became the key motivation to the pulse/pulse-reverse operations.

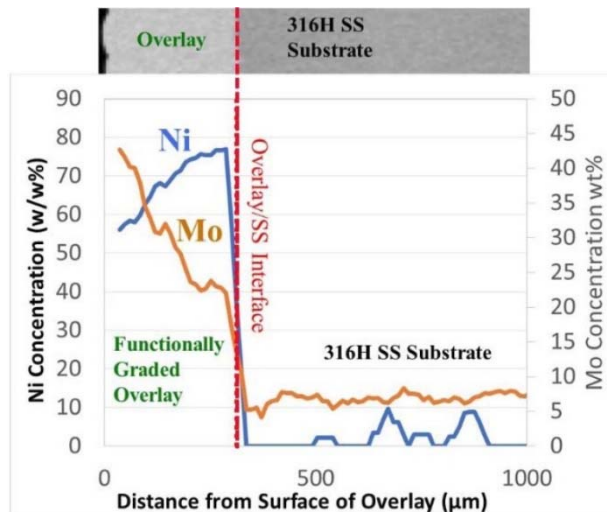


Figure 5 - EDS line scan of the functionally graded NiMo coating on a 316H SS substrate where the concentration of Ni (blue) increases from the coating surface to the interface; meanwhile the concentration of Mo (orange) decreases.

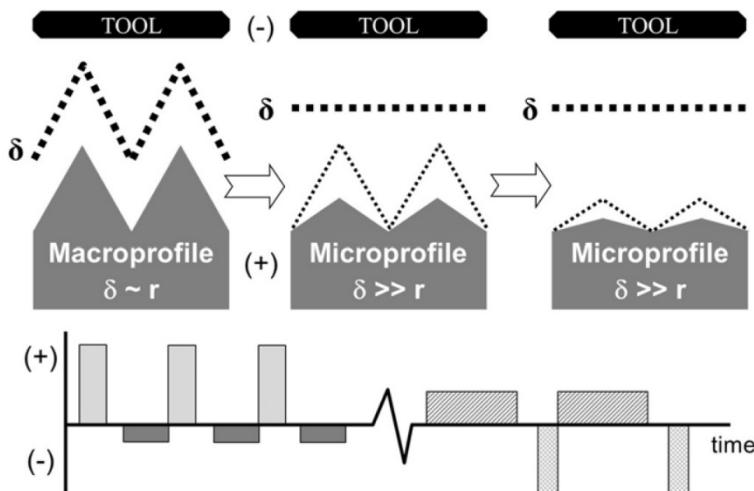


Figure 6. Schematic representation of the sequenced waveform used to electropolish stainless steel.



Figure 7 - 316SS tube surface before (top) and after (bottom) sequenced pulse reverse electropolishing in a NaCl-NaNO<sub>3</sub> electrolyte.

In our study, we initially developed finishing procedures to rapidly remove the tool lines and found that after 30 seconds of pulse/pulse reverse processing, the surface roughness stopped improving (at an  $R_a$  of ~0.2 μm (reduced from ~1 μm). This result was due to the surface finish improving to a point where the macroprofile boundary (Figure 6) no longer created enough resistance to focus the material removal on the surface peaks, per Jaquet's model (as discussed above). In order to continue to

improve the surface finish, the processing conditions needed to be adjusted to match the new boundary layer (microprofile, Figure 6) based on the finish of the surface. To achieve this, we adjusted the thickness of the boundary layer by changing the waveform parameters, and continued surface finishing (for ~15 sec) to achieve the target 0.03- $\mu\text{m}$  mirror-like finish (Figure 7). Consequently, the pulse/pulse reverse approach replaced both the AFM and the conventional DC electropolishing steps and enabled:

1. Single setup with a water based pH neutral, room temperature electrolyte.
2. Reduced total processing time from ~160 sec to 45 sec.
3. Eliminated the need for additional process controls on temperature and procurement of consumables.
4. Reduced safety and use restrictions.

### 4.2. Passivating Metal

For strongly passivating metals (titanium, niobium, tantalum and their alloys), when water-free solutions are not preferred, aggressive chemicals are commonly added to the electrolyte to remove the passive film. For example, in the case of niobium, a mixture of nine parts sulfuric and one part hydrofluoric acid is used as the electrolyte to depassivate the surface during electropolishing.<sup>5</sup> In addition to the electrolyte handling issues associated with concentrated hydrofluoric acid, conventional DC electropolishing of niobium presents process control issues, and reject rates are often 40 to 50%.<sup>6</sup> I was a part of the team at Faraday that developed a water-based pulse reverse Nb electrochemical surface finishing process that eliminates the need for low conductivity, high viscosity or HF-assisted electrolytes. The key innovation of this development was the demonstration of an approach to control the surface chemistry, such that electropolishing could occur.

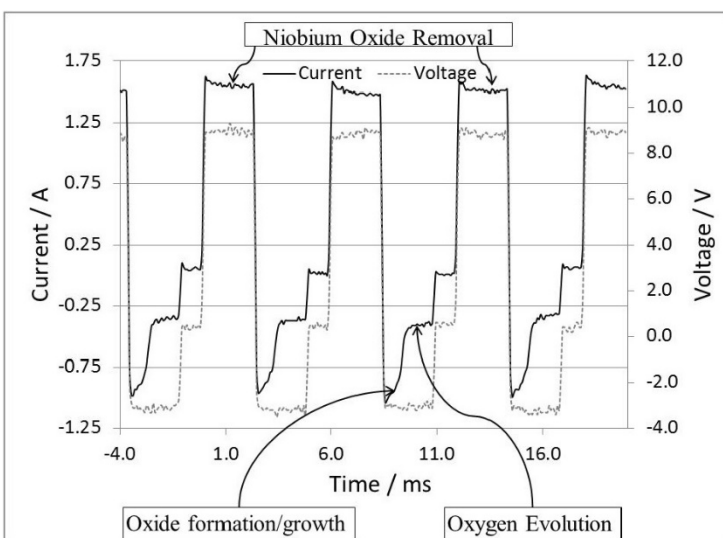


Figure 8 - Pulse reverse voltage and current response for the low frequency/low power waveform used to electropolish flat niobium coupons.



Figure 9 - Electropolished 2" x 2" tantalum coupon. Edge shows surface prior to polishing.

During the development of pulse reverse waveforms for electropolishing of niobium, effective polishing occurred when a current transition was observed in the anodic current response, as shown in Figure 8.<sup>7</sup> The pulse/pulse-reverse voltage profile was 3 V anodic for 2.5 msec/1.0 msec off-time/9 V cathodic for 2.5 msec, as confirmed with by an oscilloscope trace. Examining the resulting current profile, the anodic voltage pulse shows a transition from niobium oxide film formation to water electrolysis. Our team postulated that the high instantaneous current and rapid current decrease would be a direct result of passive oxide growth on the niobium surface. After the "complete" formation of the niobium oxide film, water electrolysis occurred during the remainder of the anodic voltage pulse. The shift from oxide formation to oxygen evolution could account for the observed anodic current transition. Further speculation suggested that the niobium oxide film was subsequently removed during the cathodic voltage pulse, resulting in a new surface for Nb oxidation. This mechanism was termed "cathodic electropolishing." A similar anodic current transition has been observed for other strongly passive materials such as tantalum (Figure 9), nickel-titanium shape memory alloys, Ti-6Al-4V, and it is anticipated that the same type of surface chemistry control occurs in these scenarios.

### 4.3. Additively Manufactured (AM) Metals

Additively manufactured metals are a special case in the surface finishing industry, due to their complex surface structure. For example, the roughness of a conventionally machined surface is 0.8 to 1.5  $\mu\text{m}$ , depending on the method by which it is machined. In the case of powder bed additively manufactured parts, the roughness can be as high as 30  $\mu\text{m}$ , with an  $R_z$  on the order 0.5 mm. To successfully electropolish these materials, a significant amount of the material needs to be removed to reach a fully dense material while maintaining the targeted geometry. Fine control of the boundary layer over complex surface contours is therefore necessary to simultaneously improve the surface finish and preserve the complex geometries that AM can produce. Furthermore, finishing of AM materials requires combining the surface finishing processes discussed above, to account for the change of both surface roughness and chemistry. Generally, as discussed below, the operating conditions need to be sequenced to achieve a nominal boundary layer control, while the pulse operating conditions need to be tuned due to the change in surface roughness and to reduce the amount of material removed.

In this example,<sup>8</sup> two waveform sequences were applied with different allotted times for electrofinishing of electron beam powder bed manufactured Ti-6Al-4V coupons. The parameters of the waveforms used in the sequences are presented in Table 1. The initial surface roughness of the coupons, as measured by  $R_a$ , was approximately 7  $\mu\text{m}$  (275  $\mu\text{in.}$ ). The waveform sequences consisted of Waveform 3 followed by Waveform 4 followed by Waveform 5. The data from Trial A are presented in Table 2. With the waveform sequence in Trial A, the initial surface roughness was 7.0/276 ( $\mu\text{m}/\mu\text{in.}$ )  $R_a$  and the final surface roughness was 1.98/78 ( $\mu\text{m}/\mu\text{in.}$ )  $R_a$ , with material removal of 664/26,141 ( $\mu\text{m}/\mu\text{in.}$ ).

Table 1 – Waveform conditions used for electropolishing additively manufactured Ti-6Al-4V.

	$V_{\text{anodic}}$ (V)	$t_{\text{anodic}}$ (msec)	$t_{\text{anodic, off}}$ (msec)	$V_{\text{cathodic}}$ (V)	$t_{\text{cathodic}}$ (msec)	$t_{\text{cathodic, off}}$ (msec)
Waveform 3	6	0.5	0	12	0.7	0
Waveform 4	6	0.3	0	12	0.6	0
Waveform 5	6	0.2	0	12	0.4	0

Table 2 – Process time with respect to the process conditions (Table 1), denoting the resulting change in surface finish and material removal.

TRIAL A	Processing Time (hr)	Initial $R_a$ ( $\mu\text{m}/\mu\text{in.}$ )	Final $R_a$ ( $\mu\text{m}/\mu\text{in.}$ )	Material Removed ( $\mu\text{m}/\mu\text{in.}$ )	Total Material Removed ( $\mu\text{m}/\mu\text{in.}$ )
Waveform 3	4	7.0/276	4.9/193	266/10472	
Plus					
Waveform 3	2	4.9/193	NA	NA	
Waveform 4	2	NA	3.7/126	233/9173	499/19645
Plus					
Waveform 4	6	3.7/126	NA	NA	
Waveform 5	2	NA	1.98/78	165/6496	664/26141
					664/26141

Based on the data obtained during Trial A, the respective time of the waveform sequence was adjusted to minimize the amount of material removed as presented in Table 3 for Trial B. With the waveform sequence in Trial B, the initial surface roughness was 6.6/260 ( $\mu\text{m}/\mu\text{in.}$ )  $R_a$  and the final surface roughness was 1.7/67 ( $\mu\text{m}/\mu\text{in.}$ )  $R_a$  with material removal of 152/5984 ( $\mu\text{m}/\mu\text{in.}$ ). By adjusting the time of the individual components of the waveform sequence, an acceptable final surface finish was achieved with approximately 23% of the material removed in Trial A.

Additional process optimization over the years has demonstrated the capability of continued refinement of the surface texture and minimizing material loss to a finish approaching 0.2  $\mu\text{m}$  (~8  $\mu\text{in.}$ ), as shown in Figure 10. The processing refinements necessary to achieve these surface finishes directly result from an improved understanding and control of the boundary layer and surface chemistry during electrochemical finishing/polishing operations.

Table 3 – The table denotes the operation time with respect to the process conditions (Table 1) and the resulting change in surface finish and material removal.

TRIAL B	Processing Time (hr)	Initial R <sub>a</sub> (μm/μin)	Final R <sub>a</sub> (μm/μin)	Material Removed (μm/μin)	Total Material Removed (μm/μin)
Plus					
Waveform 5	4	6.6/260	NA	NA	
Waveform 3	3	NA	4.8/189	71/2795	71/2795
Plus					
Waveform 4	3	NA	3.4/130	26/1023	97/3818
Plus					
Waveform 5	5.1	3.4/130	1.7/67	55/2165	152/5984
					152/5984

### 5. Concluding Remarks

The goal of my talk and this work was to demonstrate that consideration of the surface and near surface effect during electrochemical operations can have a profound impact on the performance of the material deposited or the finish of the material produced. Furthermore, the use of pulse/pulse reverse electrolysis offers the opportunity to gain even better control of the boundary layer and surface chemistry during operation.

### 6. Acknowledgement

I gratefully acknowledge the technical review of this manuscript by E.J. Taylor and Maria Inman and editorial review by James Lindsay. As this body of work is a work in-progress, I humbly acknowledge (1) past colleagues at Faraday, including Brian Skinn, Huong Le and Heather McCrabb, (2) my mentors and advisors John Zondlo, Peter Stansberry, Albert Miller, Davide Hill and Paul McGinn, (3) former and current collaborators, including Branko Popov, Kamyar Ahmadi, Jean Yves Hihn, Tim Horn, Youping Gao and Charles Arvin, and last but certainly not least, (4) current colleagues at Faraday, including Holly Garich, Stephen Snyder, Andrew Moran, Dan Wang, Rajeswaran Radhakrishnan, Santosh Vijapur, Alex Fertig, Santosh More, Victor Alderman and Katherine Lee. In addition, I acknowledge the support of various Federal Agencies for sponsored research, including the Environmental Protection Agency, the National Science Foundation, U.S. Army, U.S. Air Force, and the Department of Energy. Finally, although constrained by confidentiality requirements, I acknowledge the support and confidence of our commercial clients, customers and licensees.

As  
Received

Post  
Finished



Figure 10 - Electropolished powder bed additively manufactured Ti-6Al-4V.

### 7. References

1. P.A. Jacquet, "On the Anodic Behavior of Copper in Aqueous Solutions of Orthophosphoric Acid," *Transactions of the Electrochemical Society*, **69**, 629-655 (1936).
2. K. Ahmadi, *et al.*, *Products Finishing* (online), **84** (7), (April 2020): <https://www.pfonline.com/articles/nasfaesf-university-funded-research-transitioned-to-industry-practical-performance-improvements-in-functional-reach-compliant-trivalent-chromium-plating>.
3. K. Ahmadi, *et al.*, "Crack Free Cr Coatings from Cr 3+ Electrolyte," *J. Electrochem. Soc.*, **169** (1), 012504, (2022); DOI 10.1149/1945-7111/ac4bfa
4. T.D. Hall, R. Radhakrishnan, and H. Garich, "Functionally Graded Alloy Coating and Method for Preparation", US Patent Application # 63/502,767 (May 17, 2023).
5. H. Tian, S. Corcoran, C. Reece, M. Kelley, "The Mechanism of Electropolishing of Niobium in Hydrofluoric–Sulfuric Acid Electrolyte," *J. Electrochem. Soc.*, **155** (9), D563 (2008).
6. E.J. Taylor, private communication. Stent manufacturer, January (2011).



# The William Blum Lectures



#57 – Timothy D. Hall – 2023

7. M.E. Inman, E.J. Taylor and T.D. Hall, "Electropolishing of passive materials in HF-free low viscosity aqueous electrolytes," *J. Electrochem. Soc.*, 160 (9), E94-E98 (2013).
8. E.J. Taylor, H. Garich, H. McCrabb and T.D. Hall. "Sequenced Pulse Reverse Waveform Surface Finishing of Additively Manufactured Parts." U.S. Patent 11,118,283, Dated 09/14/21.

## 8. About the author



Dr. Timothy D. Hall is the Research Director at Faraday Technology Inc., in Clayton, Ohio. He received his B.S. in Chemical Engineering and Mathematics from West Virginia University (Morgantown, WV) in 2003, his M.S. and Ph.D. in Chemical Engineering from the University of Notre Dame (Notre Dame, IN) in 2006 and 2007, respectively. Dr. Hall was part of a team that received a 2011 R&D 100 Award, 2013 green chemistry award from the EPA and NSF, and was a 2016 R&D 100 Award finalist in both plating and surface finishing electrochemical technologies. Author of numerous scientific papers, he has been a significant contributor to work that has led to several patents and pending patent applications.